Biogeochemical effects of macroalgal decomposition on intertidal microbenthos: a microcosm experiment

E. García-Robledo, A. Corzo*, J. García de Lomas, S. A. van Bergeijk

Departamento de Biología, Facultad de Ciencias del Mar y Ambientales, Pol. Río San Pedro s/n, 11510 Puerto Real, Spain

ABSTRACT: The decomposition of macroalgal detritus (tubular and planar *Ulva* spp.) was studied in a microcosm under a daily light:dark cycle to simulate the decomposition on intertidal sediment. The consequences of bloom decay were evaluated in the bulk water phase and in the sediment. Inorganic nutrients (NO_3^-, NO_2^-, NH_4^+, PO_4^{3-} and SiO_3^{2-}), dissolved organic carbon (DOC) and inorganic carbon (DIC) were measured in the inflowing and outflowing seawater. Vertical microprofiles of O_2, pH and H_2S at the sediment–water interface, sediment contents of organic matter (OM), inorganic and organic carbon (C_{org}), total nitrogen (N) and inorganic nutrients were measured before and after addition of macroalgal detritus. Changes in the taxonomic composition of microphytobenthos were studied by optical microscopy and by the analysis of photosynthetic pigments. Macroalgal detritus vanished from the sediment surface in 6 d. Macroalgal decomposition shifted the microcosm net balance to higher releases of DOC, DIC and inorganic nutrients, suggesting rapid release from macroalgal biomass. Besides being released to the water column, a fraction of macroalgal carbon and of nitrogen was incorporated into the sediment as indicated by a transient increase in C_{org} and N. Aerobic mineralization of macroalgal detritus reduced O_2 in the water column and the sediment. Microbenthos photosynthetic activity was initially suppressed but recovered from the third day as macroalgal detritus decomposed. Photosynthetic O_2 production by microbenthos largely determined the fraction of macroalgal detritus that was aerobically mineralised. Decomposition of macroalgal detritus favoured the dominance of cyanobacteria over diatoms in the microbenthos.

KEY WORDS: Macroalgal blooms · Microbenthos · Microelectrodes · Macroalgal decomposition · Macroalgal detritus

INTRODUCTION

The progressive increase in opportunistic green macroalgal blooms is one of the most visible signs of eutrophication in coastal marine environments (Valiela et al. 1997). In temperate regions, the development of macroalgal blooms occurs mainly in spring and the bloom usually collapses and degrades in summer. Hypoxic or anoxic conditions occur frequently due to the remineralization of the bloom, leading to the accumulation of toxic sulphides and faunal mortality (Viaroli et al. 2001). Most studies have focused on the ecological conditions that trigger blooms and the impact of live mats on different ecosystem compartments and functions (Valiela et al. 1997).

Studies on bloom decay are scarce and they have focused on the decomposition of macroalgal tissue itself and also its effects in the water column, using a variety of methodological approaches. Studies of biomass losses during *in situ* incubations of live or frozen and thawed macroalgae in litter bags have demonstrated that macroalgae degrade faster than seagrasses and higher plants (likely due to their higher N-content), releasing both inorganic nutrients and organic N (Williams 1984, Buchsbaum et al. 1991, Bourgues et al. 1996). Regeneration of carbon and nitrogen in the dark has also been studied in laboratory experiments using live or pre-frozen macroalgae in oxic (Castaldelli et al. 2003) or anoxic conditions (Williams 1984, Bourgues et al. 1996). A study of decomposition of ^{14}C-labelled

Ulva rigida showed the existence of a phase of quick release of DOC during the first 15 min that was independent of bacterial activity, followed by a phase (that lasted days) of slower release dependent on bacterial activity (Castaldelli et al. 2003). Interestingly, production of organic volatile compounds during the decomposition process has been suggested (Castaldelli et al. 2003). Those experiment, either *in situ* or in the laboratory, focussed mainly on the time course of weight loss and chemical changes that occurred in the macroalgal detritus, excluding the interaction with the sediment during the decomposition process. However, decomposition frequently occurs in close contact with the sediment.

The degradation of a large amount of frozen and thawed macroalgal detritus (80 kg FW m^{-2}) in a closed mesocosms system containing a sediment layer was studied by Nedergaard et al. (2002). This system was exposed to low irradiance and quickly evolved to anoxia. Under these conditions (that typically occur in dense blooms) up to 90% of the system-integrated sulphate reduction occurs in the water column through the metabolism of thallus-associated sulphate reducers. Lomstein et al. (2006) used flow-through microcosms to quantify the nutrient and carbon release during decomposition from a macroalgae-sediment system in dark. This study confirmed the colonization of the thalli by bacteria during the decomposition process, with sulphate reducers responsible for 3% of carbon oxidation. However, sulphate reduction rates were always higher in the sediment below the macroalgae mat. The increase in C:N ratio of mineralization products (Pedersen et al. 1999) suggests that mineralised nitrogen (mainly NH$_4^+$) from the macroalgal detritus is incorporated into the bacterial biomass (Lomstein et al. 2006).

Decomposition of macroalgal blooms frequently occurs on shallow photic sediment inhabited by microphytobenthos. The degradation of macroalgal detritus is likely to affect considerably the different biogeochemical processes at the sediment–water interface. Photosynthetic activity of microphytobenthos may account for a large fraction of total primary production in estuaries and shallow environments (Underwood & Kromkamp 1999) and is an important carbon source for benthic heterotrophs (Middelburg et al. 2000). Similarly, biological activities of microbenthos play an important role in oxygen and nutrient exchange at the sediment–water interface, and therefore greatly affect the mineralization of organic matter and the biogeochemical cycling of elements in shallow environments (Risgaard-Petersen 2003 and references therein). Previous studies have considered the effects of live macroalgal mats on microbenthos (Sundbäck et al. 1996), but not the effects of macroalgal decomposition.

In addition, previous studies on decomposition have largely ignored the effects of macroalgal detritus decomposition on microbenthic community at the microscopic scale.

The aim of our study was to experimentally analyse at a microscale the biogeochemical consequences of decomposition of a macroalgal bloom on shallow sediments. We use here a microcosm approach, where the consequences of bloom decomposition on photosynthetic sediment were evaluated in the bulk water phase (dissolved organic and inorganic carbon, inorganic nutrient) and in the sediment (vertical microprofiles of O$_2$, pH, H$_2$S and inorganic nutrients, sediment content of organic matter, inorganic and organic carbon and total nitrogen). The changes in the taxonomic composition of the microphytobenthic community were also studied due to its possible effects on higher trophic levels. The duration of the experiment was long enough to encompass the decomposition of the macroalgal detritus and its subsequent fertilizing effects on the microbenthic community.

MATERIALS AND METHODS

Microcosm set-up. The sediment (upper 5 cm layer) and macroalgae were collected from muddy intertidal flats ('Río San Pedro', Cádiz Bay, Spain). The sediment was sieved (1 mm) and placed inside an aquarium (46 × 28 × 20 cm), producing a layer 6 to 7 cm thick. The aquarium was filled with 16 l of seawater collected *in situ* and filtered (5 μm), producing a water column 12 cm high. This microcosm was maintained on a 12:12 h light:dark photoperiod with continually flowing seawater (1.8 l h^{-1}; hydraulic retention time: 8 h) at 22 ± 2°C. During the light period, the aquarium was illuminated at 350 μmol photons m^{-2} s^{-1} using six 68 W fluorescent tubes (3 Grolux and 3 white lights). The microbenthic community developed over 20 d before addition of macroalgal detritus at the beginning of the experiment (Fig. 1).

The macroalgae collected included tubular *Ulva* sp. (formerly *Enteromorpha* sp., Hayden et al. 2003) and minor amounts of planar *Ulva* sp., which are common members of spring blooms in the Cádiz Bay. After collection, the macroalgal biomass was rinsed with seawater and killed by freezing at –80°C. Macroalgae were thawed immediately before being added to the aquarium. The aquarium was supplied with a total amount of 280 g FW of dead macroalgae, equivalent to an input of 220 g DW m^{-2} of macroalgal detritus. This macroalgal cover is typical in the Bay of Cádiz and lower than that reported in more eutrophic coastal areas (Viaroli et al. 2001). Before the addition of macroalgae, the microcosm was sampled to determine
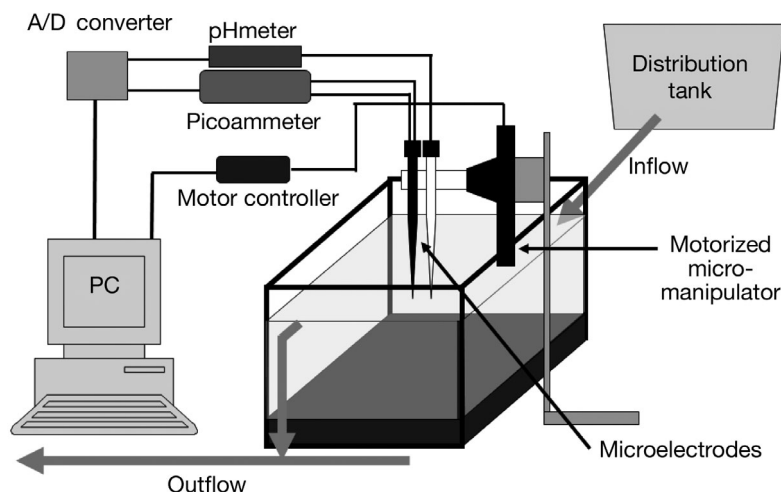
Fig. 1. Mesocosm and microelectrode set-up

initial conditions (t_0). Further sampling was done on Days 1, 3, 6, 14 and 20 after macroalgal addition. Macroscopic macroalgal detritus was excluded from the sediment samples.

Inorganic nutrients and dissolved carbon. Water samples (10 ml, n = 2) for inorganic nutrients and dissolved carbon were taken from the microcosm inflow and the outflow every sampling day and stored frozen until analysis. Inorganic nutrient (nitrate, nitrite, ammonium, phosphate and silicate) concentrations were measured using a TRAACS-800 analyzer following standard protocols (Grasshoff et al. 1983). Dissolved organic and inorganic carbon (DOC and DIC) were determined with a TOC-analyzer (Shimadzu 5050A®). Production or consumption rates for DOC, DIC and inorganic nutrients were calculated as the differences between output and input fluxes normalised to sediment surface area.

Positive and negative rates represent production and consumption, respectively. Since the aquarium was open to the atmosphere, DIC exchange is only considered in qualitative terms.

Inorganic nutrients were measured in the sediment pore water of the microcosm as follows. Six sediment cores (i.d.: 1.2 cm) were randomly collected each sampling day and frozen immediately at –80°C. Once frozen, the upper layer of each core was sliced in 7 thin sections (ca. 1 mm) using a razor blade. Sections collected from the same depth were pooled and centrifuged at 4500 rpm (1800 × g) for 30 min to extract interstitial water. Nutrient concentrations in the interstitial water were measured using a TRAACS-800 analyzer.

Nutrient fluxes across the sediment–water interface were calculated from the nutrient concentration in the bulk water phase and the linear nutrient depth profiles using the equation of Fick's first law of diffusion:

$$J(z) = - D_o \cdot [\partial C(z)/\partial z] \qquad (1)$$

where D_o is the free solution molecular diffusion coefficient of each nutrient and $[\partial C(z)/\partial z]$ is the linear nutrient concentration gradient across the sediment–water interface (up to a depth of 2 to 3 mm). D_o was used because we observed a linear gradient across the diffusive boundary layer (DBL) and the upper layer of the sediment, suggesting a very high porosity in the upper layers of the microcosm sediment. Effective DBL was determined from the O_2 profiles. D_o values for each nutrient in seawater were taken from Boudreau (1997). Positive and negative fluxes indicated net export of nutrients out of the sediment or net uptake, respectively.

Inorganic nutrient contents of macroalgae were measured after Corzo & Niell (1992). Macroalgae were dried at 70°C for 24 h and ground to an homogeneous powder. Inorganic nutrients were extracted after incubation for 2 h of 0.05 g of dry homogenised macroalgal powder in 4 ml of distilled water at room temperature. Extracts were centrifuged at 4500 rpm for 10 min and inorganic nutrients were measured in the collected supernatant using a TRAACS-800 analyser.

Organic matter, carbon and nitrogen content of sediment and macroalgae. Organic matter, carbon and nitrogen content were determined in the upper 1 cm of sediment cores (i.d.: 1.2 cm, n = 2). Organic matter was determined by loss on ignition. Total amounts of carbon and nitrogen were analyzed in dried sediment samples using a Leco CHNS 932® Analyzer. Inorganic carbon was determined in previously burned (550°C) samples and the organic fraction was determined as the difference between total and inorganic fractions.

Carbon and nitrogen content of macroalgae were determined in dried (70°C for 24 h) and ground samples with a Leco CHNS 932® Analyzer.

Vertical profiles of O_2, pH and H_2S. Vertical profiles of O_2, pH and H_2S at the sediment–water interface were measured with microelectrodes (tip diameter 20 to 30 µm, Unisense®) using the experimental set up shown in Fig. 1. The microelectrodes were mounted in pairs in a motor controlled micromanipulator (MC-232, Unisense®) connected to a PC, and were driven down into the sediment with a step resolution of 100 µm. The high-sensitivity picoammeter (Unisense PA2000®) and the high impedance mV-meter (MeterLab) were connected to a PC using an A/D converter (ACD-101, Unisense®). For each sampling day, at least 4 vertical profiles of O_2, pH and H_2S were measured. Steady-state profiles were made using the software Profix

3.05® (Unisense®). The O₂ microelectrode (Revsbech 1989) was calibrated using 100% saturation of O₂ in the air-bubbled bulk water phase of the microcosm, while 0% saturation was achieved in the anoxic layer inside the sediment. The pH microelectrode (Revsbech et al. 1983) was calibrated in 3 phosphate buffer solutions (0.1 M) of known pH (6, 8 and 10). The sulphide microelectrode was calibrated by adding known volumes of an anoxic 50 mM Na_2S stock solution in 0.1 M NaOH to a 100 mM phosphate buffer at pH 7 in anoxic conditions (Kühl et al. 1998). Oxygen fluxes across the sediment–water interface were calculated from steady state vertical profiles using Eq. (1), where D_o is the free solution molecular diffusion coefficient of O_2 and $[\partial C(z)/\partial z]$ is the linear O_2 concentration gradient across the DBL. The value of D_o was taken from Li & Gregory (1974). Additional methodological details can be found elsewhere (Corzo et al. 2005, Garcia de Lomas et al. 2005).

Pigment analysis and taxonomic composition of microbenthos. Sediment cores (i.d.: 1.2 cm, n = 6) were taken and frozen immediately at –80°C. Each core was sliced in thin sections (ca. 1 mm), which were pooled by depth, homogenised and sonicated (30 s at 15 W). Phycobiliproteins were extracted in 2 ml phosphate buffer (0.2 M, pH = 6.5) and left overnight at 4°C in darkness (Thinh 1983). Chlorophyll a was extracted in

2 ml 100% methanol (Thompson et al. 1999) and left overnight at 4°C in darkness. Extracts were centrifuged at 4500 rpm for 10 min and the absorption spectrum between 400 and 800 nm was obtained using a spectrophotometer (Unicam UV/VIS UV2®). Phycobiliproteins (phycoerythrin and phycocyanin) were estimated after Bennet and Bogorad (1973), while chl a was estimated after Pierson et al. (1987).

For taxonomic composition and abundance of microphytobenthos, the upper 5 mm of sediment cores (n = 2) were taken and fixed with glutaraldehyde (2.25% in 5 μm filtered seawater). Abundances of Cyanobacteria and diatoms were determined by light microscopy in 50 μl of a diluted (50×) and homogenised sediment suspension by counting a minimum number of 400 cells along random transects in the microscopic fields. Taxonomic identifications of microalgae were made according to Bourrelly (1970, 1981) and Boone & Castenholz (2001).

Statistical analysis. Differences over time or between depths for the measured variables were tested by 1-way and 2-way analyses of variance (ANOVA) followed by the least significant difference (LSD) method for multiple pairwise comparisons. Two means comparisons were done with the t-test method. Statistical analyses were performed using the software Statgraphics Plus 5.1.
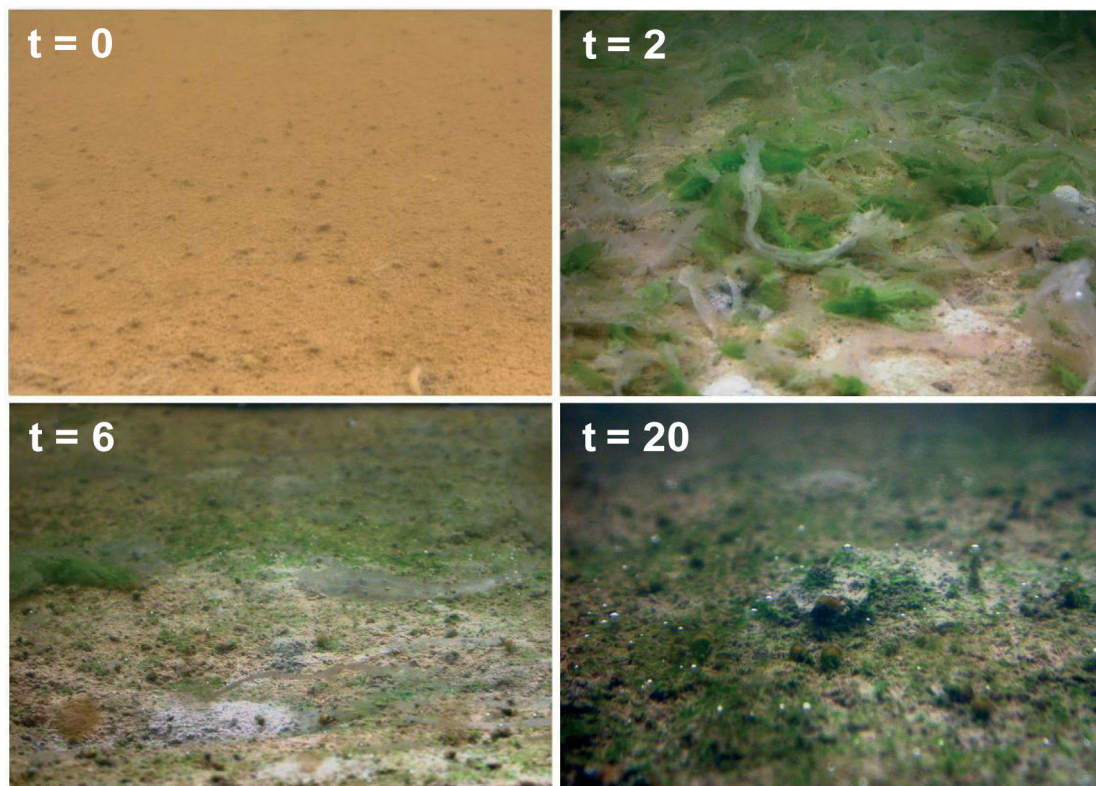

Fig. 2. Changes in the macroscopic appearance of the sediment surface in the mesocosm over 20 d (t = 1 to 20). Macroalgal detritus was added at Day t = 0 after measurements of initial conditions

RESULTS

Macroscopic description

The sediment was muddy and the surface appeared oxidised, showing a light brown colour at the initial stage (t_o). Dead macroalgae began to whiten and set-tled during the first 2 d following addition. They formed a heterogeneous layer of detritic organic mat-ter in the sediment surface leaving patches of uncov-ered sediment (Fig. 2). After 6 d, almost all of the macroalgal detritus had disappeared, and only a few small fragments remained on the sediment surface. The mineralization of macroalgal detritus appeared to stimulate the microphytobenthic community, pro-ducing a green compact biofilm on the surface of the sediment as macroalgal detritus disappeared.

Transfer of organic matter to the water column and sediment

Decomposition of macroalgal detritus released DOC to the water column as indicated by the rapid increase to more positive values in the microcosm balance for DOC after the addition of dead macroalgae (Fig. 3A). This increase was also associated with a transient shift in the microcosm balance for inorganic carbon from net negative to net positive during the first stage of decomposition (Fig. 3A).

The organic matter content of the sediment in-creased from 111.47 ± 19.25 to 206.53 ± 52.47 mg g^{-1} DW (mean $\pm$ SD, $p < 0.01$, t-test) during the first 3 d after addition of macroalgal detritus. However, the increase in OM was transitory, decreasing steadily from the 3rd day down to initial values (Fig. 3B). Organic carbon content (C_{org}) increased significantly during the first 6 d after addition of dead macroalgae (from 1.74 ± 0.01 to 2.01 ± 0.13 mmol C g^{-1} DW; mean $\pm$ SD, $p < 0.01$, t-test), then decreased steadily to the end of the experi-ment (Fig. 3C). Total nitrogen content of sediment (N) increased significantly after addition of macroal-gal detritus (0.12 ± 0.01 to 0.16 ± 0.02 mmol N g^{-1} DW at Day 6; mean $\pm$ SD, $p < 0.01$, t-test), then decreased towards the end of the experiment (Fig. 3C). The sediment C:N ratio (as C_{org}/N) increased significantly from 15.78 ± 2.41 before the addition of dead macroalgae to 19.78 ± 1.99 after 3 d (mean $\pm$ SD, $p < 0.05$, t-test) decreasing to the initial value later (Fig. 3B). Inorganic carbon content of sediment (C_{inorg}) showed a transient but signifi-cant decrease from 1.08 ± 0.05 to 0.88 ± 0.06 mmol C g^{-1} DW in the 1st day after addition of macro-algae (mean $\pm$ SD, $p < 0.01$, t-test).
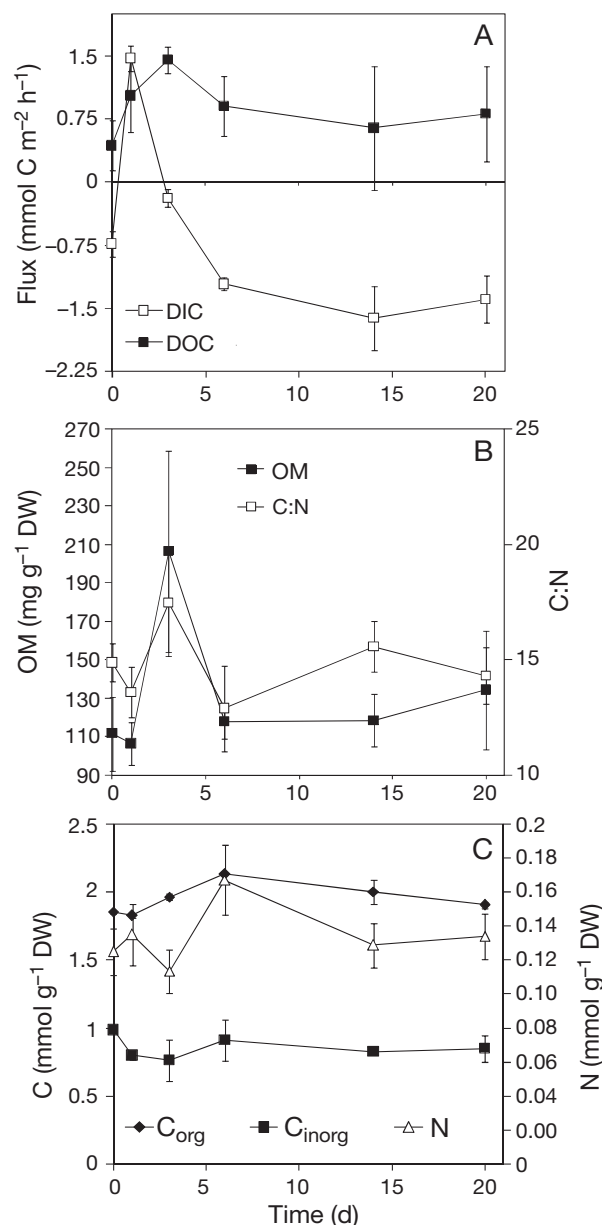

Fig. 3. (A) Microcosm mass balance (outflow–inflow) for dis-solved inorganic carbon (DIC) and dissolved organic carbon (DOC) (n = 2). (B) Changes in organic matter (OM) content (n = 2) and the organic carbon:total nitrogen ratio (C:N) of microcosm sediment (n = 4). (C) Total nitrogen (N), organic carbon (C_{org}) and inorganic carbon (C_{inorg}) content of micro-cosm sediment (n = 4). Values are means $\pm$ SD

Concentration and fluxes of inorganic nutrient

The microcosm received an important input of intra-cellular inorganic nutrient with the addition of macro-algal detritus (Table 1). NH_4^+ represented 96.5% of the intracellular inorganic nitrogen. Vertical profiles of inorganic nutrients before the addition of macroalgal detritus showed the existence of a deep layer at about

Table 1. Mean concentration ±SD (n = 2) of inorganic nutrients in the macroalgal detritus added to the microcosm, mean inorganic nutrient concentration ± SD in the inflow seawater (n = 6) and microcosm mass balance for the entire experiment taking into account the water flow velocity and the duration of the experiment (20 d). Inflow and outflow are total input and output, respectively, of nutrient in inflowing and outflowing seawater for 20 d

Nutrient	Macroalgae (μmol g^{-1} DW)	Inflow seawater (μmol l^{-1})	Macroalgae (μmol)	Inflow (μmol)	Outflow (μmol)	Balance outflow–inflow (μmol)	Balance outflow– macroalgae + inflow) (μmol)
NH_4^+	53.5 ± 4.7	1.9 ± 0.6	1132.93	1751.29	2809.78	1058.50	–74.44
NO_3^-	1.7 ± 1.0	1.5 ± 0.9	36.65	989.58	1598.18	608.60	571.95
NO_2^-	0.2 ± 0.0	0.5 ± 0.5	3.98	328.05	245.77	–82.28	–86.26
PO_4^-	11.7 ± 02	0.6 ± 0.2	247.40	483.08	523.30	40.22	–207.18
SiO_3^{2-}	1.6 ± 0.7	11.4 ± 0.3	35.05	9851.74	13074.60	3222.86	3187.80

2.5 to 4.5 mm below the sediment surface with maximum concentrations of NH_4^+, NO_3^-, NO_2^-, PO_4^{3-} and SiO_3^{2-} (Fig. 4). The deposition of macroalgae on the sediment induced a migration of the subsurface maximum of NO_3^- and SiO_3^{2-} towards to the sediment surface. However, this pattern was not observed as clearly for NH_4^+, NO_2^- and PO_4^{3-}. Maximum NH_4^+ concentrations at the sediment surface were observed on Day 6 and were coincident with a high PO_4^{3-} concentration.

Concentrations of inorganic nutrients in the bulk water were lower than those measured in sediment except for SiO_3^{2-} (Fig. 5). Net fluxes (calculated from the concentration gradient at the sediment–water interface) showed a rapid, transient increase in the net efflux of NO_3^-, which peaked at Days 1 and 3 and slowly decreased through to the end of the experiment. NH_4^+ net efflux rate increased after the addition of macroalgal detritus, peaked at Day 14 and remained high up to end of the experiment. NO_2^- and PO_4^{3-} net effluxes were lower than those of NO_3^- and NH_4^+ throughout the experiment.

The net balance of inorganic nutrients for the microcosm calculated from Eq. (1) indicated that in the initial conditions all nutrients except NH_4^+ were being consumed within the system. After the addition of macroalgae, the microcosm shifted quickly from being a net sink to a net exporter of NO_3^-, NO_2^-, PO_4^{3-} and SiO_3^{2-}. At Days 14 and 20, the system seemed to be slowly returning to the initial conditions except for SiO_3^{2-} (Fig. 5B). The total balance for 20 d indicated that the microcosm consumed NH_4^+, NO_2^- and PO_4^{3-} and released NO_3^- and SiO_3^{2-} (Table 1).

Changes in net metabolism

Oxygen concentration in the water column and within the sediment decreased quickly after the addition of macroalgal
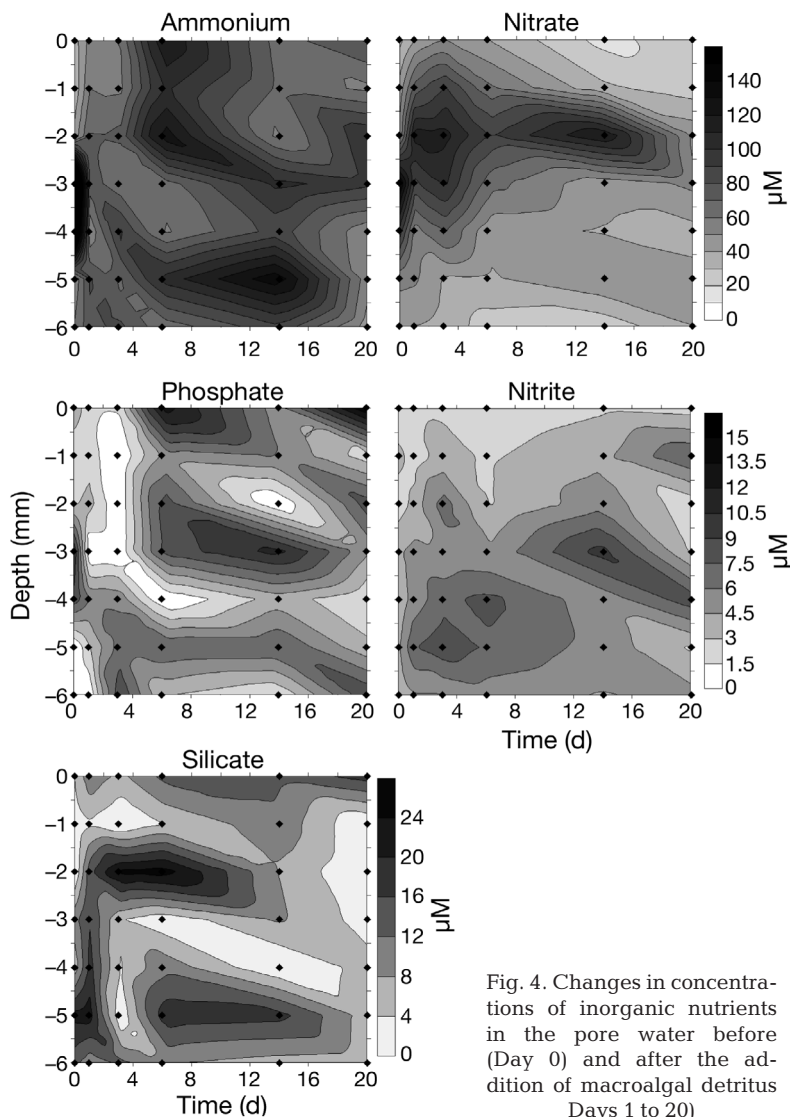

Fig. 4. Changes in concentrations of inorganic nutrients in the pore water before (Day 0) and after the addition of macroalgal detritus Days 1 to 20)
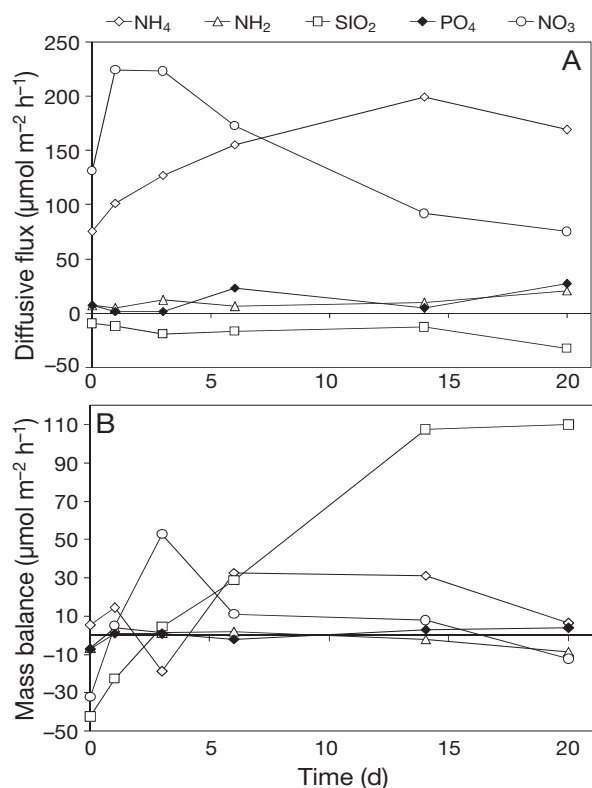
Fig. 5. (A) Fluxes of inorganic nutrients at the sediment–water interface calculated from nutrient concentration profiles in the sediment and the nutrient concentration in the bulk water phase of the microcosm. (B) Whole microcosm balance for inorganic nutrients. Positive and negative values indicate net release and net uptake, respectively, from the sediment (A) and/or the microcosm (B)

detritus. Initial oxygen concentration in the bulk water column was 215 µmol O_2 l^{-1}, decreasing to 150 µmol O_2 l^{-1} and 130 µmol O_2 l^{-1} in light and darkness, respectively, on the 3rd day (Fig. 6). Decomposition of macroalgal detritus clearly affected the oxygen concentration at the sediment–water interface. The layer
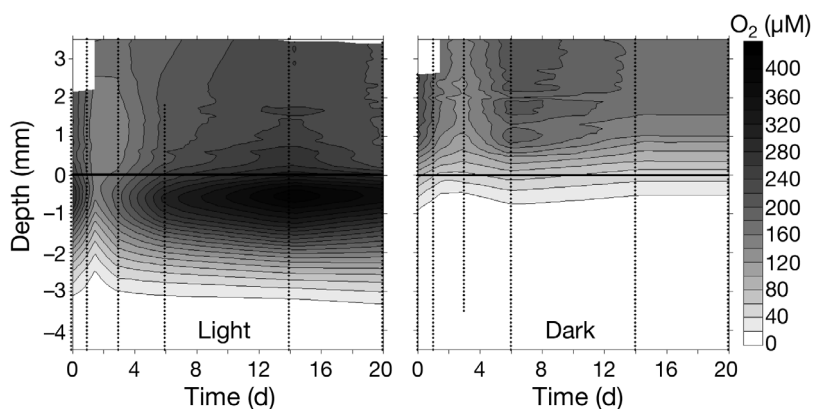

Fig. 6. Oxygen concentration in the sediment–water interface measured before (Day 0) and after addition of macroalgal detritus (Days 1 to 20) in the light and in the dark. Plotted dates of every sampling day are means of 4 to 5 O_2 profiles

of macroalgal detritus over the sediment transiently suppressed photosynthetic activity of microphytobenthos at the beginning of the experiment. Photosynthetic activity was fully recovered from Day 6. Oxygen penetration depth in the sediment decreased transiently after addition of macroalgal detritus, reaching minimum values on Day 3 (Fig. 6).

Oxygen fluxes between the sediment and the water column (calculated from O_2 microprofiles) decreased slightly (both in the light and in the dark) when the macroalgal detritus covered the sediment at the beginning of the experiment (Fig. 7A). However the differences were not significant, likely due to the heterogeneous cover of macroalgal detritus (see below). Net photosynthetic production and dark respiration started to recover from Day 3, reaching maximum values at the end of the experiment. On a daily basis, taking into account the net photosynthesis and dark respiration rates and the corresponding duration of the light and dark periods (daily net primary production), the sediment in the microcosm was net heterotrophic before the addition of macroalgal detritus but became net autotrophic towards the end of the experiment.

The sedimentation of macroalgal detritus created a considerable spatial heterogeneity in the sediment surface because it was not covered uniformly. During the first 3 to 4 d, covered and uncovered areas were clearly distinguishable (Fig. 2, t = 2). To account for the spatial heterogeneity of the cover of dead macroalgae detritus on the sediment surface, we measured O_2 profiles and the corresponding fluxes in covered and uncovered areas during the first 3 d (Fig. 7B,C). Net production rates in covered areas decreased significantly (p < 0.05, t-test) from rates of 0.42 ± 0.86 mmol O_2 m^{-2} h^{-1} to values of −0.62 ± 0.63 mmol O_2 m^{-2} h^{-1} on the 3rd day. In contrast, net production rate increased slightly (but not significantly in areas without macroalgae cover) up to 0.87 ± 0.32 mmol O_2 m^{-2} h^{-1}. Similarly, dark respiration rates decreased significantly in covered areas from values of −0.93 ± 0.12 mmol to −0.36 ± 0.22 O_2 m^{-2} h^{-1} on the 3rd day (p < 0.01, t-test). No significant differences were observed in dark respiration rates during the first 4 d in uncovered areas.

pH profiles and H_2S

Vertical profiles of pH at the sediment–water interface were closely dependent on photosynthetic activity of the microphytobenthic community, and therefore differed in the light and dark periods (Fig. 8). Initially, the mineraliza-
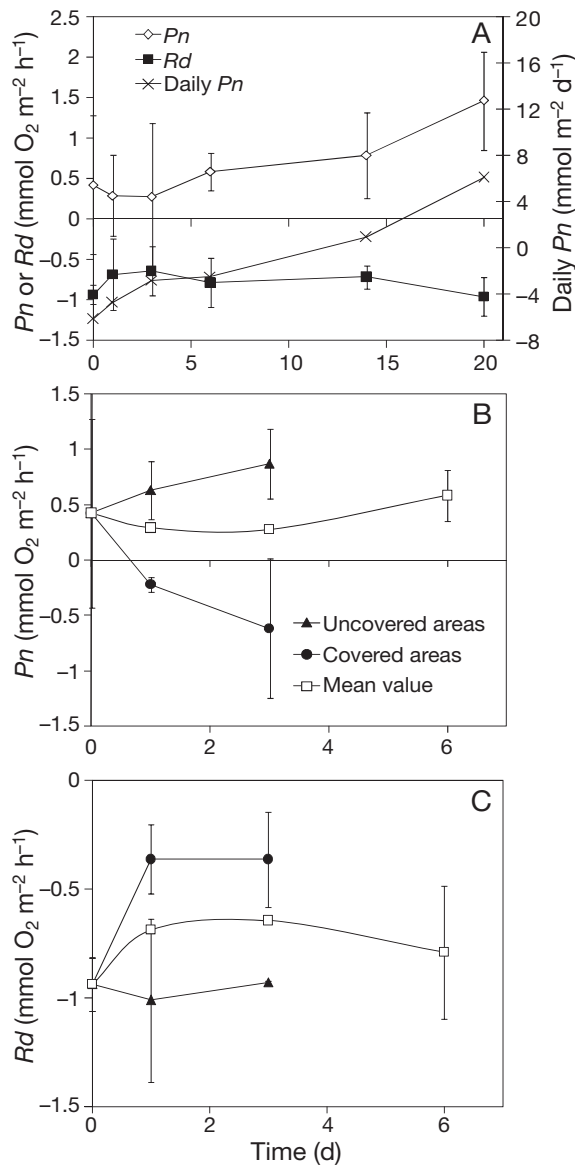
Fig. 7. Oxygen fluxes across the sediment surface. (A) Net production rates (*Pn*), respiration rates (*Rd*) and daily net production rates (Daily *Pn*). Plotted data are means of 4 or 5 profiles. (B) Spatial heterogeneity in net production rates due to presence (covered areas) and absence (uncovered areas) of macroalgal detritus during the first 3 d. Mean rates are presented for comparison. (C) Spatial heterogeneity in dark respiration rates due to presence (covered areas) and absence (uncovered areas) of macroalgal detritus during the first 3 d. *Rd* values are negative for clarity. Plotted data are means of 2 or 3 profiles. Error bars represent SDs

tion of macroalgal detritus decreased the pH in light and darkness. This decrease was observed both in the water column and within the sediment. However after the 3rd day, the microphytobenthic photosynthetic activity produced a progressively greater difference in pH between the daily periods of light and dark. Daily

pH oscillations of 1 to 2 units between the light and dark periods occurred in the water column and in the sediment (500 µm depth) at the end of the experiment (Fig. 8C,D). H_2S concentration in the upper 6 mm of sediment was frequently unmeasurable in the dark and very low in the light before and after the addition of macroalgal detritus (results not shown). At this low concentration, the known sensitivity of the H_2S microsensor to light produced erratic and unrealistic profiles for the water column and the sediment photic layer.

Microphytobenthic community

Chl *a* concentration decreased to minimum values at Day 3 (Fig. 9A). After Day 3, Chl *a* increased significantly and remained higher than at t_0 up to the end of the experiment. The sediment content of phycobiliprotein (PBP) was minimum on Day 3 and increased considerably from this day up to the end of the experiment, as did Chl *a*. However the PBP:Chl *a* ratio increased from 0.03 at t_0 to 0.06 at the end of the experiment, suggesting a stronger dominance of cyanobacteria in the photoautotrophic microbial community.

The taxonomic composition of the microphytobenthic community changed after the addition of macroalgal detritus (Table 2). Abundance of Cyanobacteria at t_0 (57%) increased further to 66%, while the abundance of diatom decreased from 43 to 34% at the end of the experiment. *Leptolyngbya* sp., *Merismopedia* sp. and *Johannesbaptistia* sp. dominated the cyanobacterial community throughout the experiment, although the abundance of *Merismopedia* sp. and particularly *Johannesbaptistia* sp. increased towards the end of the experiment. Abundant diatoms were *Nitzschia* sp., *Gyrosigma* sp., *Navicula* sp. and *Cylindrotheca* sp.

DISCUSSION

Experimental limitations

The study of decomposition requires killing macroalgae, ideally without affecting their tissular structure and degradability. As far as we know, killing by freezing is the only procedure that has been assessed so far (Buchsbaum et al. 1991, Nedergaard et al. 2002, Castaldelli et al. 2003). However no information is available on how the freeze-thaw treatment might affect the tissue structure of macroalgae and how it could affect the initial phase of the decomposition process, for instance by facilitating the release of dissolved
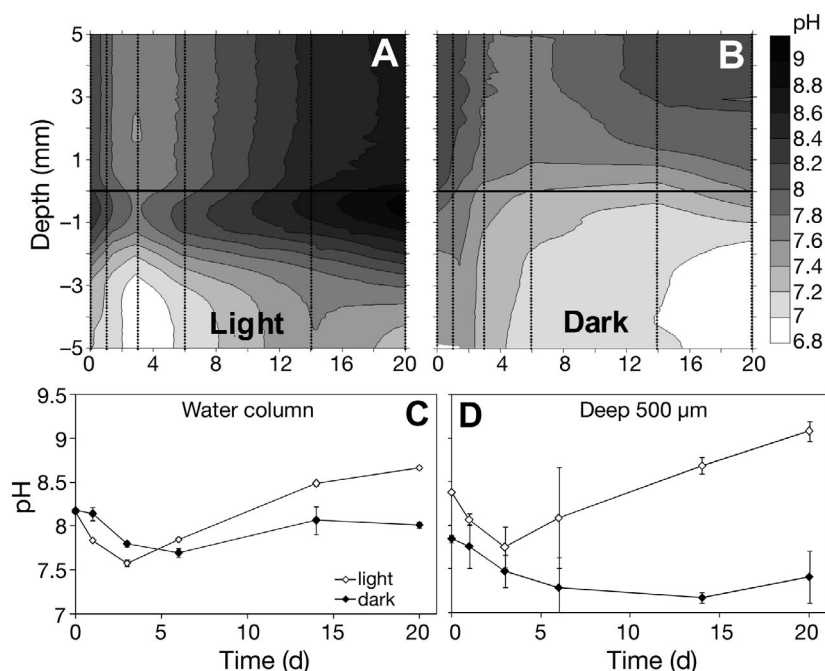
Fig. 8. pH changes at the sediment–water interface (A) in light and (B) in the dark. Plotted data are means of 2 to 4 profiles. (C) pH changes in the bulk water in the light and in the dark. (D) pH changes within the sediment (at a depth of 500 µm) in the light and in the dark. Error bars represent SDs

compounds. Likely, due to this uncertainty, some studies on decomposition chose to start with live macroalgae, inducing their senescence in the dark (Williams 1984, Lomstein et al. 2006). However, this leads to an even more complex situation where the macroalgal biomass is partially alive and partially decomposing, and this precludes the study of decomposition processes in the light. In addition, laboratory experiments have demonstrated that *Ulva* spp. and other macroalgae can survive for very long periods in the dark (Gabrielson et al. 1983, Kamermans et al. 1998). The microcosm set up can not capture the whole *in situ* complexity of the decomposition process. The

effect of macrofauna and tidal movements and associated currents that might play a role in the decomposition of macroalgae have not been considered in our experimental design.

Decomposition of macroalgae and transfer of organic matter to the water column and sediment

The decomposition of macroalgal detritus involves the rapid leaching of soluble materials in a cellular autolytic process that is independent of microbial activity. During a second phase, microbial exoenzymes continue the decomposition of labile macromolecules, leading to further release of low molecular weight DOC (Valiela et al. 1985, Castaldelli et al. 2003). These 2 phases lasted less than 1 wk, similar to previous observations (Astill & Lavery 2001, Castaldelli et al. 2003). We detected the transfer of the detrital C from macroalgae to the water column as DOC during the 1st day after the addition of macroalgal detritus, although maximum net rates were observed at Day 3 (Fig. 3A). The deposition of macroalgal detritus on the sediment surface represented an important input of C_{org} for the sediment as well (Fig. 3B). Once the macroalgal detritus settled on the sediment, a fraction of the released DOC was likely transferred to the sediment pore water. These organic compounds were relatively depleted in N since the C:N ratio increased during the initial stage of decomposition. Increases in the C:N ratios of mineralization products have also been observed in mats of senescent-decomposing macroalgae (Lomstein et al. 2006).
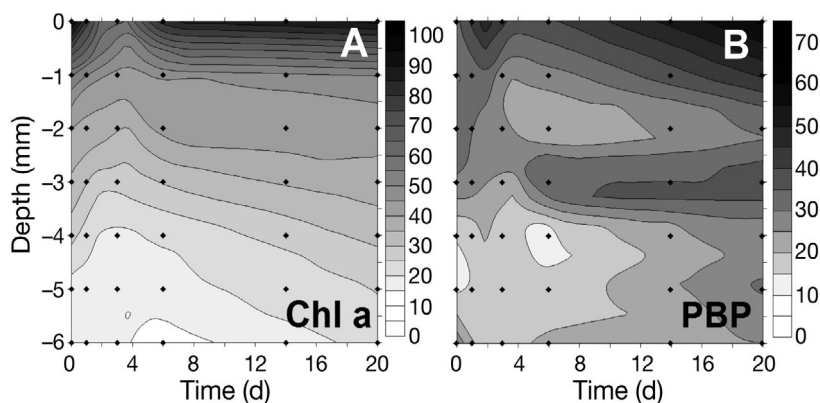
Nutrient remineralization

The addition of macroalgal detritus shifted the microcosm balance for all measured nutrients to net production (Fig. 5). Initially, NO_3^- and NH_4^+ may have been released from intracellular pools since green macroalgae accumulate these nutrients in large concentrations (Corzo & Niell 1992). However, the total amounts of intracellular NO_3^- and NH_4^+ introduced with macroalgal detritus were 37 and 1133 µmol respectively (Table 1). This relatively small amount of

Fig. 9. Vertical profiles of (A) chl *a* and (B) phycobiliproteins (phycoerythrin and phycocyanin)

Table 2. Changes in taxonomic composition of the microphytobenthic community. Values are means ± SD (n = 2) before (t_0) and 20 d after addition of macroalgae (t_{20}). Values in brackets are percentages of the whole community

| | Cell ($\times 10^5$) ml^{-1} (%) | |
	t_0	t_{20}
Cyanobacteria		
Leptolyngbya sp.	4.80 ± 0.93 (55.60)	2.88 ± 0.62 (43.06)
Merismopedia sp.	0.07 ± 0.02 (0.83)	0.10 ± 0.09 (1.56)
Johannesbaptistia sp.	0.05 ± 0.01 (0.58)	0.71 ± 1.00 (21.25)
Spirulina sp.	0.01 ± 0.02 (0.13)	0
TOTAL	4.93 ± 0.96 (57.14)	3.69 ± 1.53 (65.86)
Diatoms		
Nitzschia sp.	0.54 ± 0.76 (6.25)	0
Gyrosigma sp.	0.83 ± 0.13 (9.58)	0.27 ± 0.11 (3.97)
Navicula sp.	0.40 ± 0.23 (4.68)	0.35 ± 0.09 (5.24)
Cylindrotheca sp.	0.20 ± 0.04 (2.33)	0
Entomoneis sp.	0.18 ± 0.03 (2.02)	0.28 ± 0.00 (4.25)
Unidentified	1.06 ± 0.94 (12.24)	1.40 ± 0.03 (23.45)
TOTAL	3.70 ± 1.19 (42.86)	2.28 ± 0.07 (34.14)
TOTAL	8.64 ± 0.23	5.97 ± 1.46

NO_3^- can explain the change in the microcosm's balance during only the 1st day, but not the extra NO_3^- efflux up to Day 3. In addition, we observed only a small NH_4^+ efflux, which peaked at the final stage of decomposition (Day 6). Therefore, intracellular NH_4^+ released during the initial phase of decomposition must have been partially transformed to NO_2^- and NO_3^- by nitrification, or consumed by benthic microalgae and/or heterotrophic bacteria. This NH_4^+ input likely reduced the competition between heterotrophic bacteria and nitrifiers, thus producing an increase in nitrification rates (Strauss & Lamberti 2000, Risgaard-Petersen 2003). The increase in NO_3^- production rate and the reduction of its consumption rate by microphytobenthos produced a transient increase in NO_3^- concentration in the porewater that induced a transient efflux to the water column. The initial nitrate efflux may also be caused by a displacement of the nitrification zone upward in the sediment following the decrease in oxygen penetration depth (Fig. 4). A clear increase in the NH_4^+ content of sediment was only observed at Day 6, and it was likely due to ammonification activity on macroalgal organic nitrogen (Fig. 4). During this phase and later, the microphytobenthic community had recovered photosynthetic activity and was growing (Figs. 6, 7 & 9). Assimilation of NH_4^+ by microphytobenthos has been suggested to control the NH_4^+ efflux from the sediment, and likely plays a role in the net flux of NO_3^- as well (Sundbäck & Snoeijs 1991, Dalsgaard 2003). Calculated NO_3^- and NH_4^+ fluxes at the sediment–water interface were in general higher than those obtained from the microcosm balance, but followed the same general trends (Fig. 5),

and were within the range of published values (Risgaard-Petersen 2003, Sundbäck et al. 2004, Eyre & Ferguson 2005). Disparities between calculated and measured diffusive fluxes are frequently observed, and likely stem from biological processes and methodological procedures. Net fluxes of PO_4^{3-} and NO_2^- were much lower than those of NO_3^- and NH_4^+. This was true even when the intracellular PO_4^{3-} input with macroalgal detritus was relatively high (247 µmol) compared with the intracellular NO_2^- input (4 µmol). This suggests a strong PO_4^{3-} consumption rate during the initial decomposition phase since we detected high PO_4^{3-} concentrations within the sediment only after Day 6 (Fig. 4). The bacterial community was likely the major consumer of PO_4^{3-} during the first 3 d because photosynthetic activity and growth by benthic microalgae were inhibited (Figs. 6, 7 & 9). Our results are contradictory for SiO_3^{2-}. According to the total microcosm balance, SiO_3^{2-} was exported from the microcosm after Day 3, while the calculated fluxes across the sediment–water interface and the shape of the vertical profiles within the sediment suggest that there was a net flux from the water to the sediment throughout the experiment. Calculated fluxes across the sediment–water interface are based in a number of assumptions (Boudreau 1997) that might not have been fulfilled for SiO_3^{2-}, although they worked reasonably well for other nutrients in same experiment. Clearly the microcosm was a large net source of SiO_3^{2-} (more than 3 mmol over 20 d, Table 1). This SiO_3^{2-} must have originated from within the sediment through a process triggered by macroalgal decomposition.

Effect of macroalgal detritus on the microbenthos net metabolism

Since *Rd* was higher than *Pn* (Fig. 7B,C), sediment metabolism before the addition of macroalgal detritus was net heterotrophic, according the benthic trophic state index (BTSI) proposed by Rizzo et al. (1996). The sedimentation of macroalgal detritus likely reduced incident light at the sediment surface, as has been shown for live macroalgal mats (Astill & Lavery 2001). However, the patchy cover of macroalgal detritus produced large horizontal variation in the light reaching the sediment surface. Photosynthetic O_2 production was almost completely suppressed in covered patches

and increased in the uncovered areas (Fig. 7B). Uncovered patches had net O_2 production rates double those within the covered areas. This, increase is likely the consequence of the fertilization produced by the rapid release of the inorganic nutrient during the mineralization of macroalgal detritus in nearby covered patches. In the covered patches, light was insufficient to sustain photosynthetic activity and the metabolism of the microbenthic community shifted to fully heterotrophic (according to BTSI). However this inhibition was transient. Photosynthetic O_2 production in light began to recover after 3 d as macroalgal detritus progressively disintegrated, shifting net metabolism of microbenthic community once more from net heterotrophic (Day 6) to net autotrophic (Days 14 and 20).

O$_2$ availability for the sediment was decreased by the presence of the macroalgal detritus because: (1) it represented a physical barrier for mass transfer between the sediment and the bulk water phase, and (2) O_2 was being consumed within the macroalgal detritus layer (Pedersen et al. 1999, Nedergaard et al. 2002). This likely explains the decrease of the aerobic respiration rates in covered patches while it remained similar to initial values in uncovered patches (Fig. 7C).

Aerobic/anaerobic mineralization of macroalgal detritus

The transient accumulation of C_{org} and the hypoxic-anoxic conditions should have favoured sulfate reduction activity. High levels of sulfate reduction activity have been measured in thalli of decomposing *Ulva lactuca* in anoxic conditions (Nedergaard et al. 2002) and in sediments below senescent mats of microcosms (Lomstein et al. 2006). However, we did not detect a significant increase in the H_2S after the addition of macroalgal detritus. This could be partially due to the relatively low load of macroalgal detritus added in our experiment compared to previous studies. In addition, H_2S concentration can be buffered at very low levels in sediments with high Fe content even when rates of sulfate reduction activity are high (Canfield et al. 1992, Kasten & Jørgensen 2000) like those of Cádiz Bay (12 to 26 mg Fe g^{-1} FW, J. Blasco unpubl. data).

The aerobic oxidation of C_{org} lead to a decrease in pH (Fig. 8), likely shifting the balance between precipitation and dissolution to dissolution of carbonate minerals (Mucci et al. 2000). The decrease in C_{inor} content of sediment during the first 3 d (Fig. 3C) was probably driven by the decrease in pore water pH (Fig. 8). This is a clear signal that macroalgal decomposition might transiently alter the capacity of intertidal sediment to sequester C in inorganic forms. The anaerobic oxidation of C_{org} by sulfate reduction should increase pH and alkalinity, increasing the saturation state of carbonates and favouring precipitation (Mucci et al. 2000). We observed a slight increase in C_{inorg} from Day 3 that was coincident with a change in pH of the microcosm water column and within the sediment in light (Figs. 3C & 8). Daily changes in O_2 availability and O_2 penetration depth in the sediment, together with the photosynthetically driven daily changes in pH, likely affect the overall C_{org} and C_{inorg} preservation rates of decaying macroalgal blooms in intertidal sediments (Kristensen et al. 1995, Holmer 1999).

Changes in the microphytobenthic community and fertilization

The initial microphytobenthic biomass in the microcosm estimated by chl *a* concentration was in the low to middle range of published *in situ* values (Cahoon 1999). We observed an immediate transient decrease after the addition of macroalgal detritus (Fig. 9A). Below a dense macroalgal canopy, irradiance may be too low to support photosynthetic activity and therefore chlorophyll synthesis by the microphytobenthos (Sundbäck et al. 1996, Astill & Lavery 2001). However, at the macroalgal detritus load used in our experiment, this only occurred in the covered patches (Fig. 7). In addition to a transient decrease in chl *a* concentration, we observed taxonomic changes in the microphytobenthic community not previously reported (Table 2). Microphytobenthos was slightly dominated by filamentous colonial Cyanobacteria like *Leptolyngbya* sp., *Merismopedia* sp. and *Johannesbaptistia* sp. These species are generally scarce in typical intertidal sediments, where benthic diatoms usually dominate the community due to a higher grazing resistance (Cahoon 1999, Garcia de Lomas et al. 2005). The relative increase of Cyanobacteria after the addition of macroalgal detritus was likely due to their higher resistance to anoxic conditions than diatoms (Cohen et al. 1986, De Wit et al. 1988) and their higher capacity for using organic substrates (Stal & Moezelaar 1997). The environmental conditions were probably less favourable for diatom growth (Admiraal & Peletier 1979), although the utilization of organic substrate by some diatoms has been reported as well (Nilsson & Sundbäck 1996, Tuchman et al. 2006). In addition, low stoichiometric Si:N and Si:P ratios in the pore water were more favourable for Cyanobacteria. The degradation of macroalgal detritus further enriched the system in N and P in relation to Si availability. Likely, these conditions favoured further cyanobacterial growth and hence their dominance in the microbial community. Interestingly, the mesocosm shifted from being a net sink for Si to a net source (Fig. 5B), sug-

gesting the existence of a net flux from the sediment to the water column that was not fully intercepted by the benthic diatom assemblage. The observed shift in the taxonomic composition of the microphytobenthic community might affect higher trophic levels. The degradation of macroalgal detritus in photic sediments released organic and inorganic compounds that provided energy and materials sources for the microbenthic community, leading in turn to the transient fertilization of the sediment. Increases in nutrients stimulated the phototrophic community, increasing photosynthetic activity and biomass.

LITERATURE CITED

Admiraal W, Peletier H (1979) Sulphide tolerance of benthic diatoms in relation to their distribution in an estuary. Br Phycol J 14:185–196

Astill H, Lavery PS (2001) The dynamics of unattached benthic macroalgal accumulations in the Swan-Canning estuary. Hydrol Process 15:2387–2399

Bennett A, Bogorad L (1973) Complementary chromatic adaptation in a filamentous blue-green alga. J Cell Biol 58:419–435

Boone DR, Castenholz RW (2001) Bergey's manual of systematic bacteriology. 2nd edn, Vol 1. The Archeae and the deeply branching and phototrophic Bacteria. Springer, New York

Boudreau BP (1997) Diagenetic models and their interpretation: modelling transport and reactions in aquatic sediments. Springer, Berlin

Bourgues S, Auby I, Wit R, Labourg PJ (1996) Differential anaerobic decomposition of seagrass (*Zostera noltii*) and macroalgal (*Monostroma obscurum*) biomass from Arcachon Bay (France). Hydrobiologia 329:121–131

Bourrelly P (1970) Les algues d'eau douce. Initiation à la systématique. I: Les algues bleues et rouges, les eugléniens, peridiniens et cryptomonadines. Boubée, Paris

Bourrelly P (1981) Les algues d'eau douce. Initiation à la systématique. III: Les algues jaunes et brunes. Chrysophycées, phéophycées, xanthophycées et diatomées. Boubée, Paris

Buchsbaum R, Valiela I, Swain T, Dzierzeski M, Allen SD (1991). Available and refractory nitrogen in detritus of coastal vascular plants and macroalgae. Mar Ecol Prog Ser 72:131–143

Cahoon LB (1999) The role of benthic microalgae in neritic ecosystem. Oceanogr Mar Biol Annu Rev 37:47–86

Canfield DE, Raiswell R, Bottrell J (1992) The reactivity of sedimentary iron minerals toward sulfide. Am J Sci 292:659–683

Castaldelli G, Welsh DT, Flachi G, Zucchini G, Colombo G, Rossi R, Fano EA (2003) Decomposition dynamics of the bloom forming macroalga *Ulva rigida* C.Agardh determined using a ^{14}C-carbon radio-tracer technique. Aquat Bot 75:111–122

Cohen Y, Jorgensen BB, Revsbech NP, Poplawski R (1986) Adaptation to hydrogen sulfide of oxygenic and anoxygenic photosynthesis among Cyanobacteria. Appl Environ Microbiol 51:398–407

Corzo A, Niell FX (1992) Inorganic nitrogen metabolism in *Ulva rigida* illuminated with blue light. Mar Biol 112: 223–228

Corzo A, Garcia de Lomas J, van Bergeijk SA, Luzon A, Mayayo MJ, Mata P (2005) Carbonate mineralogy along a biogeochemical gradient in recent lacustrine sediments of Gallocanta Lake (Spain). Geomicrobiol J 22:283–298

Dalsgaard T (2003) Benthic primary production and nutrient cycling in sediments with benthic microalgae and transient accumulation of macroalgae. Limnol Oceanogr 48:2138–2150

De Wit R, Van Boekel WHM, Van Gemerden H (1988) Growth of the cyanobacterium *Microcoleus chthonoplastes* on sulphide. FEMS Microbiol Ecol 53:203–209

Eyre BD, Ferguson AJP (2005) Benthic metabolism and nitrogen cycling in a subtropical east Australian estuary (Brunswick): temporal variability and controlling factors. Limnol Oceanogr 50:81–96

Gabrielson JO, Birch PB, Hamel KS (1983) Decomposition of *Cladophora.* Part II. In vitro studies of nitrogen and phosphorus regeneration. Bot Mar 25:173–179

Garcia de Lomas J, Corzo A, García C, van Bergeijk SA (2005) Microbenthos in a hypersaline tidal lagoon: factors affecting microhabitat, community structure and mass exchange at the sediment–water interface. Aquat Microb Ecol 38:53–69

Grasshoff K, Ehrhardt M, Kremling K (1983) Methods of sea water analysis. Verlag Chemie, Weinheim

Hayden HS, Blomster J, Maggs CA, Silva PC, Stanhope MJ, Waaland JR (2003) Linnaeus was right all along: *Ulva* and *Enteromorpha* are not distinct genera. Eur J Phycol 38:277–294

Holmer M (1999) The effect of oxygen depletion on anareobic organic matter degradation in marine sediment. Estuar Coast Mar Sci 48:383–390

Kamermans P, Malta EJ, Verschuure JM, Lentz LF, Schrijvers L (1998) Role of cold resistance and burial for winter survival and spring initiation of an *Ulva* spp. (Chlorophyta) bloom in a eutrophic lagoon (Veerse Meer lagoon, The Netherlands). Mar Biol 131:45–51

Kasten S, Jørgensen BB (2000) Sulfate reduction in marine sediments. In: Schultz HD, Zabel M (eds) Marine geochemistry. Springer, Bremen

Kristensen E, Ahmed SI, Devol AH (1995) Aerobic and anaerobic decomposition of organic matter in marine sediments: which is faster? Limnol Oceanogr 40:1430–1437

Kühl M, Steuckart C, Eicker G, Jeroschewski P (1998) A H_2S microsensor for profiling biofilms and sediments: application in an acidic lake sediment. Aquat Microb Ecol 15: 201–209

Li YH, Gregory S (1974) Diffusion of ions in deep-sea sediments. Geochim Cosmochim Acta 38:703–714

Lomstein BA, Guldberg LB, Neubauer ATA, Hansen J and others (2006) Benthic decomposition of *Ulva lactuca*: a controlled laboratory experiment. Aquat Bot 85:271–281

Middelburg JJ, Barranguet C, Boschker HTS, Herman PMJ, Moens T, Heip CHR (2000) The fate of intertidal microphytobenthos carbon: an *in situ* C-13-labeling study. Limnol Oceanogr 45:1224–1234

Mucci A, Sundby B, Gehlen M, Arakaki T, Zhong S, Silverberg N (2000) The fate of carbon in continental shelf sediments of eastern Canada: a case of study. Deep-Sea Res II 47:733–760

Nedergaard RI, Risgaard-Petersen N, Finster K (2002) The importance of sulfate reduction associated with *Ulva lactuca* thalli during decomposition: a mesocosm experiment. J Exp Mar Biol Ecol 275:15–29

Nilsson C, Sundbäck K (1996) Amino acid uptake in natural microphytobenthic assemblages studied by microautoradiography. Hydrobiologia 332:119–129

Pedersen AU, Berntsen J, Lomstein BA (1999) The effect of eelgrass decomposition on sediment carbon and nitrogen cycling: a controlled laboratory experiment. Limnol Oceanogr 44:1978–1992

Pierson B, Oesterle A, Murphy GL (1987) Pigments, light penetration, and photosynthetic activity in the multi-layered microbial mats of Great Sippewissett salt marsh, Massachusetts. Microb Ecol 45:365–376

Revsbech NP (1989) An oxygen microelectrode with a guard cathode. Limnol Oceanogr 34:474–478

Revsbech NP, Jørgensen BB, Blackburn TH, Cohen Y (1983) Microelectrode studies of photosynthesis and O_2, H_2S and pH profiles of a microbial mat. Limnol Oceanogr 28: 1062–1074

Risgaard-Petersen N (2003) Coupled nitrification-denitrification in autotrophic and heterotrophic estuarine sediments: on the influence of benthic microalgae. Limnol Oceanogr 48:93–105

Rizzo WM, Dailey SK, Lackey GJ, Christian RR, Berry BE, Wetzel RL (1996) A metabolism-based trophic index for comparing the ecological values of shallow-water sediment habitats. Estuaries 19:247–256

Stal LJ, Moezelaar R (1997) Fermentation in cyanobacteria. FEMS Microbiol Rev 21:179–211

Strauss EA, Lamberti GA (2000) Regulation of nitrification in aquatic sediments by organic carbon. Limnol Oceanogr 45:1854–1859

Sundbäck K, Snoeijs P (1991) Effects of nutrient enrichment on microalgal community composition in a coastal shallow-water sediment system: an experimental study. Bot Mar 34:341–358

Sundbäck K, Carlson L, Nilsson C, Jönsson B, Wulff A, Odmark S (1996) Response of benthic microbial mats to drifting green algal mats. Aquat Microb Ecol 10:195–208

Sundbäck K, Linares F, Larson F, Wulff A (2004) Benthic oxygen fluxes along a depth gradient in a microtidal fjord: the role of denitrification and microphytobenthos. Limnol Oceanogr 49:1095–1107

Thinh LV (1983) Effect of irradiance on the physiology and ultrastructure of marine cryptomonad, *Cryptomonas strain Lis* (Cryptophyceae). Phycologia 22:7–11

Thompson RC, Tobin ML, Hawkins SJ, Norton TA (1999) Problems in extraction and spectrophotometric determination of chlorophyll from epilithic microbial biofilms: towards a standard method. J Mar Biol Assoc UK 79: 551–558

Tuchman NC, Schollet MA, Rier ST, Geddes P (2006) Differential heterotrophic utilization of organic compounds by diatoms and bacteria under light and dark conditions. Hydrobiologia 561:167–177

Underwood GJC, Kromkamp J (1999) Primary production by phytoplankton and microphytobenthos in estuaries. Adv Ecol Res 29:93–153

Valiela I, Teal JM, Allen SD, Van Etten R, Goehringer D, Volkmanm S (1985) Decomposition in salt marsh ecosystems: the phases and major factors affecting disappearance of above-ground organic matter. J Exp Mar Biol Ecol 89:29–54

Valiela I, McClelland J, Hauxwell J, Behr PJ, Hersh D, Foreman K (1997) Macroalgal blooms in shallow estuaries: controls and ecophysiological and ecosystem consequences. Limnol Oceanogr 42:1105–1118

Viaroli P, Azzoni R, Bartoli N (2001) Evolution of the trophic conditions and dystrophic outbreaks in the Sacca di Goro lagoon (Northern Adriatic Sea). In: Faranda FM (ed) Structure and process in the Mediterranean ecosystems. Springer-Verlag, Milan, p 340–355

Williams SL (1984) Decomposition of the tropical macroalga *Caulerpa cupressoides* (West) C. Agardh: field and laboratory studies. J Exp Mar Biol Ecol 80:109–124